

## High Angular Momentum Components in the Subbarrier Fusion of Heavy Ions

P. J. Nolan, D. J. G. Love, A. Kirwan, and D. J. Unwin  
*Oliver Lodge Laboratory, University of Liverpool, Liverpool L69 3BX, United Kingdom*

and

A. H. Nelson and P. J. Twin  
*Daresbury Laboratory, Daresbury, Warrington WA4 4AD, United Kingdom*

and

J. D. Garrett  
*Niels Bohr Institute, University of Copenhagen, 2100 Copenhagen Ø, Denmark,  
and Daresbury Laboratory, Daresbury, Warrington WA4 4AD, United Kingdom*  
(Received 11 March 1985)

The fusion of  $^{80}\text{Se} + ^{80}\text{Se}$  has been studied near and just below the Coulomb barrier. High angular momentum components were observed by measurement of  $\gamma$ -ray multiplicity distributions for the decay of the evaporation residues.

PACS numbers: 25.70.Jj

More than a decade ago it was established that the energy dependence of fusion-evaporation cross sections is not reproduced by statistical-model decay calculations.<sup>1,2</sup> In particular, they predict too rapid a decrease in cross sections for specific evaporation residues with increasing incident (or compound-nucleus excitation) energy. For example, when light Er or Yb isotopes are formed with an excitation energy of about 55 MeV, about 1% of the reaction cross section is observed in the  $1n$  evaporation residue.<sup>3</sup> Such cross sections are about two orders of magnitude larger than those of the observed high-energy  $\gamma$ -ray decays associated with giant resonances based on states of large angular momentum<sup>4</sup> which would populate in the  $1n$  channel, and represent even larger discrepancies with standard decay calculations. More recently, such enhanced cross sections for  $^{154}\text{Er}$ , the product of the  $^{92}\text{Zr}(^{64}\text{Ni}, 2n)$  reaction, have been attributed<sup>5</sup> to a "superdeformed" shape populated by the near-symmetric entrance channel which survives sufficiently long to influence the neutron and  $\gamma$ -ray decay of the systems.

Considerable attention has also been focused on near-barrier fusion cross sections, where for some systems, enhancements are observed<sup>6,7</sup> relative to single-dimensional barrier penetration calculations. Such enhanced fusion cross sections recently have been attributed<sup>8</sup> to coupling to inelastic and transfer channels. These couplings also lead to enhanced cross sections for evaporation residues corresponding to fewer emitted neutrons and to greatly enhanced partial-wave cross sections for large angular momenta.<sup>9</sup> That is, such couplings provide an alternative explanation to that proposed by Kuhn *et al.*<sup>5</sup> for the hinderance of neutron emission from compound systems,

with the consequence that a broad partial-wave cross-section distribution would be populated in the evaporation residues. Indeed, high  $\gamma$ -ray multiplicities associated with large partial-wave cross sections have been observed for  $^{166}\text{Yb}$ , the dominant evaporation residue of the  $^{154}\text{Sm} + ^{16}\text{O}$  reaction even at near-threshold energies.<sup>10</sup> Results have also been obtained<sup>11</sup> on the decay of the  $^{160}\text{Er}$  compound nucleus populated in a range of reactions,  $^{80}\text{Se} + ^{80}\text{Se}$ ,  $^{123}\text{Sb} + ^{37}\text{Cl}$ ,  $^{96}\text{Zr} + ^{64}\text{Ni}$ , and  $^{144}\text{Nd} + ^{16}\text{O}$ , near and just above threshold energies. In this case it was concluded that the average angular momentum transfer depends on the asymmetry of the entrance channel, higher angular momenta being observed in the near-symmetric systems, and the results were interpreted in terms of ground-state zero-point vibrations. Similarly, detailed measurements of the  $\gamma$ -ray multiplicity distribution have been compared with statistical decay calculations at energies well above the fusion barrier.<sup>12</sup> Systematic detailed measurements of the  $\gamma$ -ray multiplicity distributions near and below the barrier remain to be made.

The present Letter reports such measurements for the  $^{80}\text{Se} + ^{80}\text{Se}$  system using TESSA2,<sup>13</sup> an array of fifty bismuth germanate (BGO) detectors approaching a solid angle of  $4\pi$  sr surrounded by six Compton-suppressed germanium detectors. Preliminary reports of this work have appeared in recent conference proceedings.<sup>14</sup> The measurements were made with use of thin  $100\text{-}\mu\text{g}\text{-cm}^{-2}$  targets of  $^{80}\text{Se}$  (isotopic enrichment 98%) on gold backings. The  $^{80}\text{Se}$  beam was provided by the NSF tandem accelerator at Daresbury Laboratory. The energies used, 255, 260, 265, 270, 280, 290, 300, and 310 MeV, extend from well below to well above the classical Coulomb barrier of 270

MeV. The target thickness was chosen so that the beam-energy spread across the target was small ( $\sim 2$  MeV). Evaporation residues were identified and the  $\gamma$ -ray multiplicity of their decays measured by use of TESSA2. The high resolution and good peak-to-total efficiencies of the Compton-suppressed germanium detectors allow even weak transitions (and hence reaction channels) to be identified. This feature is essential to clearly identify  $\gamma$  rays associated with the various fusion channels as the fusion cross section drops experimentally by two orders of magnitude between 300 and 260 MeV. The BGO detector measures for individual reaction events the sum energy, which is related to total  $\gamma$ -ray energy, and the fold, which is related to the multiplicity, of the  $\gamma$ -ray shower. The sum energy versus fold (the number of BGO detectors triggered in a particular event) distributions for the  $2n$ ,  $3n$ , and  $4n$  products at a beam energy of 280 MeV are shown in Fig. 1. Also shown is the corresponding distribution for Coulomb-excitation events which dominate the germanium-detector spectra. This portion of the sum-energy-fold space has been excluded from the subsequent analysis.

The total fold distributions shown in Fig. 2 were derived by projection onto the fold axis and then addition of the spectra corresponding to the  $2n$ ,  $3n$ ,  $4n$ , and  $5n$  channels. Over the beam-energy range used (255–310 MeV) these channels account for the vast majority of the evaporation-residue cross section, e.g.,  $> 99\%$  below 290 MeV,  $> 95\%$  at 300 MeV, and

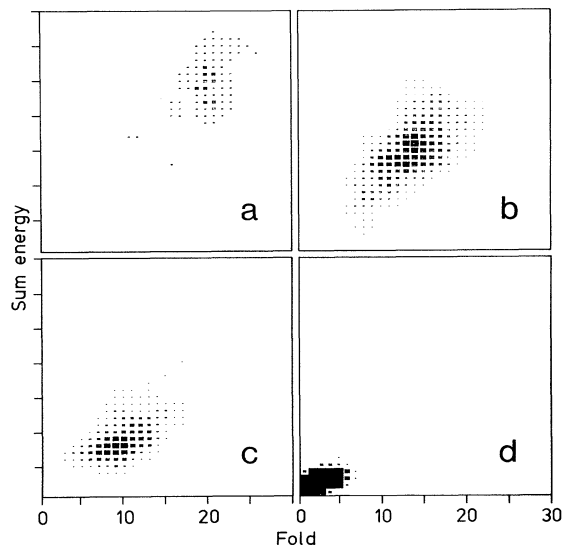


FIG. 1. Sum energy against fold distributions following the  $^{80}\text{Se} + ^{80}\text{Se}$  reaction at 280 MeV. The spectra shown are in coincidence with (a) the 334-keV  $\gamma$  ray in  $^{158}\text{Er}$  ( $2n$ ), (b) the 415-keV  $\gamma$  ray in  $^{157}\text{Er}$  ( $3n$ ), (c) the 344-keV  $\gamma$  ray in  $^{156}\text{Er}$  ( $4n$ ), (d) Coulomb excitation.

$> 92\%$  at 310 MeV. The  $2n$  distributions are also shown in Fig. 2, indicating that the high-fold components arise, as expected, from the channels with the minimum number of particles evaporated. The multiplicity scale indicated on Fig. 2 was obtained by use of the fold-to-multiplicity conversion function determined for TESSA2 with use of  $\gamma$ -ray sources.<sup>13</sup> The data have not been unfolded to account for the response of the BGO detector; hence this scale is not applicable to the extreme tails of the fold distributions. However, the multiplicities corresponding to the centroids of the distributions obtained for the heaviest evaporations residues are well determined. These are given in Table I with the experimental fold centroids. The conversion from multiplicity to angular momentum requires a knowledge of the multipolarity of the  $\gamma$ -ray transitions involved. The heavier evaporation residues populated in this work ( $^{158,157}\text{Er}$ ) are known to be good rotors to very high spin, and our angular distribution data ( $30^\circ/90^\circ$  ratio) confirm that  $> 90\%$  of the intensity arises from stretched quadrupoles. Therefore, we choose the conversion between  $M_\gamma$  and angular momentum  $I$  which has been established experimentally for heavier rotational erbium nuclei<sup>15</sup> in the range  $9 \leq M_\gamma \leq 23$ , i.e.,  $I = 2(M_\gamma - 4)$ , where  $M_\gamma$  is the multiplicity.

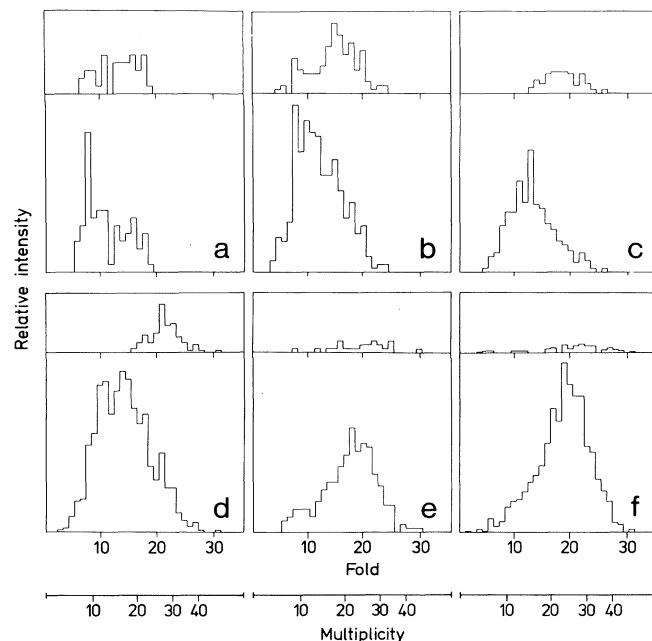


FIG. 2. Fold distributions following the  $^{80}\text{Se} + ^{80}\text{Se}$  reaction. For each energy the sum of contributions from the  $2n$ ,  $3n$ ,  $4n$ , and  $5n$  channels are shown together with the  $2n$  distribution alone. The data are taken at various beam energies: (a) 260, (b) 265, (c) 270, (d) 280, (e) 300, (f) 310 MeV. The multiplicity scale shown is taken from the measured fold-multiplicity response for TESSA2 (see text).

TABLE I. Centroids of the fold and multiplicity distributions for the  $2n$  and  $3n$  evaporation residues. Errors are given in brackets.

| Beam energy (MeV) | Compound nucleus excitation energy (MeV) | Relative cross section <sup>a</sup> | Fold                       |                            | Multiplicity <sup>b</sup>  |                            | Angular momentum <sup>c</sup> ( $\hbar$ ) |                            |
|-------------------|--|-------------------------------------|----------------------------|----------------------------|----------------------------|----------------------------|---|----------------------------|
|                   |  |                                     | $2n$ ( $^{158}\text{Er}$ ) | $3n$ ( $^{157}\text{Er}$ ) | $2n$ ( $^{158}\text{Er}$ ) | $3n$ ( $^{157}\text{Er}$ ) | $2n$ ( $^{158}\text{Er}$ )                | $3n$ ( $^{157}\text{Er}$ ) |
| 255               | 38.0                                     | ...                                 | 12(2)                      | ...                        | 15(3)                      | ...                        | 22(6)                                     | ...                        |
| 260               | 40.5                                     | 1.0(0.3)                            | 12.5(0.6)                  | ...                        | 15.7(1.1)                  | ...                        | 23(2)                                     | ...                        |
| 265               | 43.0                                     | 4.7(0.5)                            | 14.1(0.4)                  | ...                        | 18.0(1.0)                  | ...                        | 28(2)                                     | ...                        |
| 270               | 45.5                                     | 10.2(0.8)                           | 17.1(0.3)                  | ...                        | 22.3(1.2)                  | ...                        | 37(2)                                     | ...                        |
| 280               | 50.5                                     | 35(3)                               | 20.6(0.4)                  | ...                        | 28.2(1.5)                  | ...                        | 48(3)                                     | ...                        |
| 290               | 55.5                                     | ...                                 | 20(2)                      | ...                        | 27(3)                      | ...                        | 46(6)                                     | ...                        |
| 300               | 60.5                                     | 100(2)                              | 19.6(1.2)                  | 18.6(0.4)                  | 26(2)                      | 24.8(1.4)                  | 44(4)                                     | 45(3)                      |
| 310               | 65.5                                     | ...                                 | 19.8(1.0)                  | 20.0(0.2)                  | 27(2)                      | 27.2(1.4)                  | 46(4)                                     | 49(3)                      |

<sup>a</sup>Derived from sum of  $2n$ ,  $3n$ ,  $4n$ , and  $5n$  channels and normalized to 100 at 300 MeV.

<sup>b</sup>Uncertainty in the fold-to-multiplicity conversion is  $\pm 5\%$ .

<sup>c</sup>The ground-state spin of  $^{133}_{2}$  has been included in the angular momenta given for the  $3n$  channel.

It is clear from the data that high-angular-momentum components are present in the fusion of  $^{80}\text{Se} + ^{80}\text{Se}$  even below the classical fusion barrier of  $E_{\text{lab}} \approx 270$  MeV. In order to determine whether such cross sections are anomalously large, the results will be compared with the partial cross-section distribution for barrier penetration. If the fusion-barrier radius,  $R_B$ , and curvature,  $\hbar\omega_0$ , are assumed to be independent of angular momentum,<sup>16</sup> the partial-wave distribution of cross sections,  $\sigma_l(E)$ , corresponding to the penetration of a parabolic approximation<sup>17</sup> to the sum of Coulomb, nucleus-nucleus, and angular-momentum potentials becomes particularly simple and takes the form

$$\sigma_l(E) = \frac{\pi}{k^2} \frac{(2l+1)}{1 + e^{\alpha} e^{l(l+1)/\gamma^2}},$$

where

$$\alpha = (2\pi/\hbar\omega_0)(V_B - E)$$

and

$$\gamma^2 = \hbar\omega_0\mu R_B^2/\pi\hbar^2.$$

$V_B$  is the fusion-barrier height,  $\mu$  is the reduced mass,  $k$  the wave number,  $E$  the beam energy, and  $l$  the angular momentum. With the assumption of the exponential form of the nucleus-nucleus potential,<sup>18</sup>  $R_B = 12.0$  fm,  $\hbar\omega_0 = 4.04$  MeV, and thus  $\gamma = 13.3$ , then for energies well below the fusion barrier the partial-wave distribution approaches

$$\sigma_l(E) = (\pi/k^2)(2l+1)e^{-\alpha}e^{-l(l+1)/\gamma^2}$$

as a limit. The shape of this distribution, which is in-

dependent of energy, is shown in Fig. 3.

Even within the uncertainties associated in the conversion of the measured fold to multiplicity and angular momentum, the measured subbarrier cross-section distribution extends to significantly larger angular momenta than the limiting distribution. This effect probably corresponds to an effective lowering of the fusion barrier associated with the coupling of inelastic or transfer degrees of freedom as suggested by Landowne and Dasso.<sup>9</sup> Such measured multiplicity (angular momentum) distributions in the vicinity of the fusion barrier provide a more sensitive test of both the effects of additional reaction channels and the details of the nucleus-nucleus potential than total-fusion measurements.

This work is supported by the U. K. Science and Engineering Research Council. Three of us (A.K.,

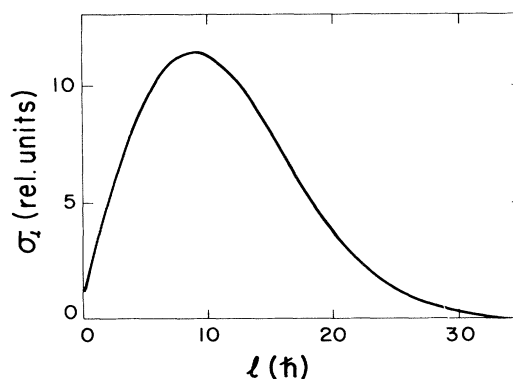


FIG. 3. Partial-wave cross-section distribution, i.e.,  $(2l+1) \exp[-l(l+1)/\gamma^2]$ , for the fusion of  $^{80}\text{Se} + ^{80}\text{Se}$  in the subbarrier limit.

D.J.U., and A.H.N.) acknowledge the receipt of Science and Engineering Research Council postgraduate studentships during this work. Discussions with D. Brink, C. Dasso, S. Landowne, and N. Rowley are acknowledged.

---

<sup>1</sup>J. Gilat, E. R. Jones, and J. M. Alexander, Phys. Rev. C **7**, 1973 (1973).

<sup>2</sup>S. Della Negra, H. Lauvin, H. Jungelass, Y. Le Beyec, and M. Lefort, Z. Phys. A **282**, 75 (1977).

<sup>3</sup>C. Cabot, S. Della Negra, H. Lauvin, Y. Le Beyec, and M. Lefort, in *Proceedings of the International Conference on Nuclear Structure, Tokyo, 1977* (International Printing, Tokyo, 1977), p. 668.

<sup>4</sup>J. O. Newton *et al.*, Phys. Rev. Lett. **46**, 1383 (1981).

<sup>5</sup>W. Kuhn, P. Chowdhury, R. V. F. Janssens, T. L. Khoo, F. Hass, J. Kasagi, and R. H. Ronningen, Phys. Rev. Lett. **51**, 1858 (1983).

<sup>6</sup>M. Beckerman *et al.*, Phys. Rev. Lett. **45**, 1472 (1980). M. Beckerman, M. Salomao, A. Sperduto, J. D. Molitons, and A. Di Rienzo, Phys. Rev. C **25**, 837 (1982).

<sup>7</sup>R. G. Stockstad and E. E. Gross, Phys. Rev. C **23**, 281 (1981), and references therein.

<sup>8</sup>C. H. Dasso, S. Landowne, and A. Winther, Nucl. Phys. **A405**, 381 (1983), and **A407**, 221 (1983).

<sup>9</sup>S. L. Landowne and C. H. Dasso, Phys. Lett. **138B**, 32 (1984).

<sup>10</sup>R. Vandenbosch, B. B. Back, S. Gil, A. Lazzarini, and A. Ray, Phys. Rev. C **28**, 1161 (1983).

<sup>11</sup>B. Hass *et al.*, Phys. Rev. Lett. **54**, 398 (1985).

<sup>12</sup>D. G. Sarantites *et al.*, Phys. Lett. **115B**, 441 (1982).

<sup>13</sup>P. J. Twin, P. J. Nolan, R. Aryaeinejad, D. J. G. Love, A. H. Nelson, and A. Kirwan, Nucl. Phys. **A409**, 343c (1983); P. J. Twin, C. Kalfas, P. J. Nolan, D. J. G. Love, A. H. Nelson, A. Kirwan, D. Howe, P. D. Forsyth, J. F. Sharpey-Schafer, and B. M. Nyako, in *Proceedings of the Twelfth International Winter Meeting, Bormio, 1984*, edited by I. Iori (University of Milan, Milan, Italy, 1984), p. 476.

<sup>14</sup>P. J. Nolan, in Proceedings of the Fifth Adriatic Nuclear Physics Conference, Hvar, Yugoslavia, 24–29 September 1984 (to be published).

<sup>15</sup>B. Herskind, in Proceedings of the Symposium on Macroscopic Features in Heavy-Ion Collisions, Argonne, 1976, Argonne National Laboratories Report No. PHY-76-2 (unpublished), Vol. 1, p. 385, and private communication.

<sup>16</sup>C. Y. Wong, Phys. Rev. Lett. **31**, 766 (1973).

<sup>17</sup>T. D. Thomas, Phys. Rev. **116**, 703 (1959).

<sup>18</sup>P. R. Christensen and A. Winther, Phys. Lett. **65B**, 19 (1976).